DALTON

Variable-temperature nuclear magnetic resonance spectroscopic studies of the dynamic behaviour of the mixed-metal cluster compounds $[MM'Ru_4H_2(\mu\text{-dppf})(CO)_{12}]$ [M = M′ = Cu, Ag or Au; M = Cu, M′ = Au; dppf = $Fe(\eta^5\text{-}C_5H_4PPh_2)_2$] and the crystal structures of $[MM'Ru_4H_2(\mu\text{-dppf})(CO)_{12}]$ (M = Cu or Au, M′ = Au)*,†

Ian D. Salter,[a] Vladimir Šik,[a] Steven A. Williams[a] and Trushar Adatia[b]

[a] *Department of Chemistry, University of Exeter, Exeter EX4 4QD, UK*
[b] *School of Chemistry, University of North London, London N7 8DB, UK*

The free energies of activation ($\Delta G^{\ddagger}$) for the fluxional processes in the clusters $[M_2Ru_4H_2(\mu\text{-dppf})(CO)_{12}]$ [M = Cu **1**, Ag **2** or Au **3**; dppf = 1,1′-bis(diphenylphosphino)ferrocene] have been determined by band-shape analysis of variable-temperature ^1H or $^{31}P\text{-}\{^1H\}$ NMR spectra. In solution, the dppf ligand attached to the coinage metals in each of **1**–**3** undergoes dynamic behaviour involving inversion at the phosphorus atoms, together with twisting of the cyclopentadienyl rings, and values of 47.0 ± 0.2, 51.5 ± 0.1 and 48.8 ± 0.2 kJ mol^{-1} were obtained for $\Delta G^{\ddagger}$ of this fluxional process in **1**–**3**, respectively. The metal cores of these three clusters are also stereochemically non-rigid in solution and values of $\Delta G^{\ddagger}$ of 47.7 ± 0.2 and 39.9 ± 0.4 kJ mol^{-1} have been calculated for a coinage-metal site-exchange process in **1** and **2**, respectively. The new trimetallic cluster $[AuCuRu_4(\mu_3\text{-}H)_2(\mu\text{-dppf})(CO)_{12}]$ **4**, which is closely related to the bimetallic clusters **1**–**3**, has been synthesized in *ca.* 40% yield by treating $[Cu_2Ru_4(\mu_3\text{-}H)_2(\mu\text{-dppf})(CO)_{12}]$ with the complex $[AuCl(SC_4H_8)]$. Variable-temperature ^1H NMR studies on **4** demonstrate that the dppf fluxion still occurs in solution ($\Delta G^{\ddagger}$ 49.2 ± 0.2 kJ mol^{-1}), but the metal skeleton of the cluster is stereochemically rigid, which is in marked contrast to those of the bimetallic analogues **1**–**3**. The structures of $[MM'Ru_4H_2(\mu\text{-dppf})(CO)_{12}]$ (M = Cu or Au, M′ = Au) have been established by single-crystal X-ray diffraction studies. The metal framework of **4** consists of a tetrahedron of ruthenium atoms with one face capped by the copper atom and one $CuRu_2$ face of the $CuRu_3$ tetrahedron so formed is capped by the gold atom to give an overall capped trigonal-bipyramidal metal-core geometry [Cu–Au 2.641(1), Cu–Ru 2.755(1)–2.909(2), Au–Ru 2.780(1) and 2.815(1), Ru–Ru 2.783(1)–2.998(1) Å]. The other two $CuRu_2$ faces are capped by triply bridging hydrido ligands, the dppf ligand bridges the two coinage metals and each ruthenium atom is bonded to three terminal CO groups. The skeletal geometry of **3** is reasonably similar to that of **4**, with a second gold atom replacing the copper atom. However, one of the Au–Ru distances [3.558(2) Å] is too long for any significant bonding interaction between the two metal atoms, so the metal framework of **3** is somewhat distorted towards a capped square-pyramid [Au–Au 2.901(1), Au–Ru 2.771(1)–2.846(1), Ru–Ru 2.775(2)–3.016(1) Å]. As observed for **4**, the bidentate diphosphine ligand bridges the two Group 11 metals in **3** and each ruthenium atom is bonded to three terminal CO groups, but one of the hydrido ligands bridges a Ru–Ru vector rather than capping an $AuRu_2$ face.

The synthesis, characterization and dynamic behaviour in solution of the novel mixed-metal cluster compounds $[M_2Ru_4H_2(\mu\text{-dppf})(CO)_{12}]$ [M = Cu **1**, Ag **2** or Au **3**; dppf = 1,1′-bis(diphenylphosphino)ferrocene] have recently been reported.[2] A single-crystal X-ray diffraction study on the copper-containing cluster **1** showed that the metal-core structure consists of a tetrahedron of ruthenium atoms capped by a copper atom, with one of the $CuRu_2$ faces of the $CuRu_3$ tetrahedron so formed further capped by a second copper atom. Thus, the overall skeletal geometry of **1** is a capped trigonal bipyramid with two distinct copper sites. Spectroscopic data strongly suggest that the silver- and gold-containing clusters **2** and **3** adopt similar metal-core structures to that observed for **1**. However, the possibility that the capped trigonal-bipyramidal metal framework of **3** is distorted towards a capped square-based pyramidal skeletal geometry could not be excluded on the evidence available.[2] In solution, each of the clusters **1**–**3** exhibits two distinct fluxional processes.[2] First, the metal frameworks of all three clusters undergo dynamic behaviour involving exchange of the coinage metals between the two distinct sites, even though the two Group 11 metals are linked together by the bidentate diphosphine ligand dppf. Secondly, at room temperature, the dppf ligand attached to the coinage metals in each of the clusters **1**–**3** is also stereochemically non-rigid in solution and it undergoes a fluxional process which involves inversion at the phosphorus atoms, together with twisting of the cyclopentadienyl rings. The skeletal rearrangement and the fluxional behaviour of the dppf ligand were found to be definitely independent for clusters **2** and **3**. Only one other example of a dppf ligand, which bridges two metal atoms in a cluster, undergoing similar dynamic behaviour to that observed for **1**–**3** has previously been reported.[3] It is interesting that this dppf fluxion in the cluster $[Au_2Ru_4(BH)(\mu\text{-dppf})(CO)_{12}]$ is reported to be in concert with a 'rocking' motion of the two gold atoms with respect to the Ru_4B core and the two processes were found to be mutually dependent,[3] which is in marked contrast to the situation observed for **2** and **3**.[2]

* The Heteronuclear Cluster Chemistry of the Group 1B Metals. Part 20.[1]

† Basis of the presentation given at Dalton Discussion No. 1, 3rd–5th January 1996, University of Southampton, UK.

However, it is possible that the dppf ligand in $[Ru_3(\mu\text{-dppf})(CO)_{10}]$ also exhibits the same type of fluxional behaviour as that for **1**–**3**. There are four distinct cyclopentadienyl (cp) hydrogen environments in the ground-state structure of the cluster, but the ^1H NMR spectrum is reported to show only two cp multiplet signals (4 H each). The authors do not comment on the ^1H NMR spectrum and no information about the multiplicity of the peaks or the values of the coupling constants is given.[4] In view of the novelty of the fluxional behaviour of the bridging dppf ligand, we wished to investigate it further by determining the free energies of activation ($\Delta G^{\ddagger}$) for the process in clusters **1**–**3** to discover to what extent the type of coinage metal that the bidentate diphosphine ligand is bonded to affects the magnitude of $\Delta G^{\ddagger}$. We also wanted to establish whether or not the dppf fluxion will occur in a cluster with a stereochemically rigid metal skeleton, because of the mutual dependence of the process and fluxional behaviour of the metal core reported[3] for $[Au_2Ru_4(BH)(\mu\text{-dppf})(CO)_{12}]$. Therefore, we wished to synthesize the new trimetallic cluster $[AuCuRu_4(\mu_3\text{-}H)_2(\mu\text{-dppf})(CO)_{12}]$ **4**, which is closely related to the bimetallic species **1**–**3**, and to study the dynamic behaviour of the dppf ligand by variable-temperature ^1H NMR spectroscopy. It was anticipated that the metal framework of cluster **4** would not undergo a Group 11 metal site-exchange process in solution, because the metal core of the analogous cluster $[AuCuRu_4(\mu_3\text{-}H)_2\{\mu\text{-}Ph_2P(CH_2)_2PPh_2\}(CO)_{12}]$ **5** has been previously reported[5] to be stereochemically rigid in solution.

In addition, some previous studies[6] on the series of clusters $[M_2Ru_4H_2(\mu\text{-}L_2)(CO)_{12}]$ [M = Ag or Au; $L_2 = Ph_2P(CH_2)_nPPh_2$ (n = 1–6) or *cis*-$Ph_2PCH{=}CHPPh_2$], which are closely related to **1**–**3**, have revealed an interesting link between changes in the metal-core geometries of the gold-containing species and the values of $\Delta G^{\ddagger}$ for the coinage-metal site-exchange process in the silver-containing species. The bidentate diphosphines $Ph_2P(CH_2)_nPPh_2$ (n = 1 or 2) and *cis*-$Ph_2PCH{=}CHPPh_2$, which distort the metal cores of the gold-containing clusters from the favoured capped trigonal-bipyramidal structure to or towards a capped square-based pyramidal geometry, are also associated with low values of $\Delta G^{\ddagger}$ for the skeletal-rearrangement process when they are attached to the silver atoms in the analogous silver-containing clusters. This correlation has been interpreted[6] as indirect evidence in support of a restricted Berry pseudo-rotation mechanism for the Group 11 metal site-exchange process in capped trigonal-bipyramidal metal frameworks of this type of cluster. In view of the above results, we were interested in performing a single-crystal X-ray diffraction study on the gold-containing cluster **3** to establish its solid-state structure and to assess whether the observed skeletal geometry can also be linked to the value of $\Delta G^{\ddagger}$ measured for the coinage-metal site-exchange process in the analogous silver-containing cluster **2**.

Examples of single-crystal X-ray diffraction studies on cluster compounds with a dppf ligand bridging two metal atoms[2,4] and on Group 11 metal heteronuclear clusters containing more than one type of coinage metal[7] are both relatively rare. Therefore, we also wished to perform a single-crystal X-ray diffraction study on the trimetallic cluster $[AuCuRu_4(\mu_3\text{-}H)_2(\mu\text{-dppf})(CO)_{12}]$ **4**.

Results and Discussion

Synthesis and spectroscopic characterization of the new trimetallic cluster $[AuCuRu_4(\mu_3\text{-}H)_2(\mu\text{-dppf})(CO)_{12}]$ 4

Treatment of a dichloromethane solution containing an excess of the bimetallic cluster $[Cu_2Ru_4(\mu_3\text{-}H)_2(\mu\text{-dppf})(CO)_{12}]$ **1** with a dichloromethane solution of the complex $[AuCl(SC_4H_8)]$ affords the trimetallic species $[AuCuRu_4(\mu_3\text{-}H)_2(\mu\text{-dppf})(CO)_{12}]$ **4** in *ca.* 40% yield. A very small amount of the bimetallic gold-containing cluster $[Au_2Ru_4(\mu_3\text{-}H)(\mu\text{-}H)(\mu\text{-dppf})(CO)_{12}]$ **3**, in which both copper atoms initially present in the starting material have been replaced, was also produced in the reaction. The IR spectrum in the carbonyl region of a sample of **3** produced in the above metal-exchange reaction is identical to the data quoted in the literature.[2]

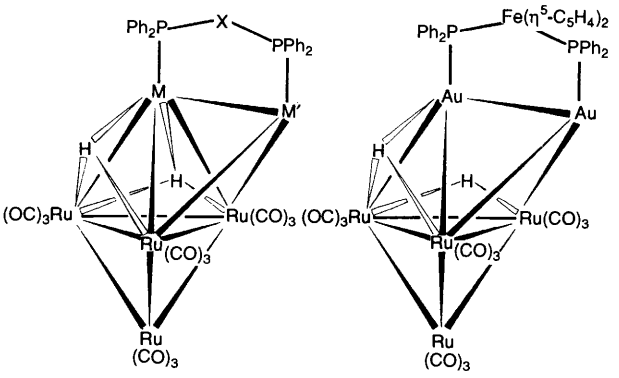

	M	M′	X
1	Cu	Cu	$Fe(\eta^5\text{-}C_5H_4)_2$
2	Ag	Ag	$Fe(\eta^5\text{-}C_5H_4)_2$
4	Cu	Au	$Fe(\eta^5\text{-}C_5H_4)_2$
5	Cu	Au	$(CH_2)_2$

3

The microanalysis, the IR spectrum and the ^1H and $^{31}P\text{-}\{^1H\}$ NMR spectroscopic data for cluster **4** are fully consistent with the proposed formulation. The IR spectrum of **4** in the carbonyl region is closely similar to that reported for the analogous cluster $[AuCuRu_4(\mu_3\text{-}H)_2\{\mu\text{-}Ph_2P(CH_2)_2PPh_2\}(CO)_{12}]$ **5**, suggesting that **4** adopts a very similar capped trigonal-bipyramidal metal-core structure to that established by a single-crystal X-ray diffraction study for **5**.[5] At −80 °C, two hydrido ligand signals and eight resonances for the cyclopentadienyl hydrogens are observed in the ^1H NMR spectrum of cluster **4**. These signals are entirely consistent with a ground-state structure in which the dppf ligand adopts a conformation with respect to a capped trigonal-bipyramidal metal skeleton which is similar to that previously observed for the copper-containing bimetallic cluster **1**.[2] The magnitudes of the $^{31}P\text{-}^1H$ couplings (11 and 14 Hz) observed for the two doublets due to the hydrido ligands in the ^1H NMR spectrum of **4** at −80 °C are very similar to those previously reported for the low-temperature ^1H NMR spectrum of the $Ph_2P(CH_2)PPh_2$ analogue **5** (12 and 13 Hz),[5] which again suggests a close similarity between the structures adopted by **4** and **5**. The proposed structure of **4** has been confirmed by a single-crystal X-ray diffraction study, but detailed discussion of these results is best deferred until the data from the variable-temperature NMR spectroscopic studies have been presented.

Variable-temperature NMR spectroscopic studies of the dynamic behaviour of the clusters $[MM'Ru_4H_2(\mu\text{-dppf})(CO)_{12}]$ (M = M′ = Cu, Ag or Au; M = Cu, M′ = Au) in solution

The energy parameters for the fluxional process, which the dppf ligand attached to the clusters **1**–**3** undergoes in solution, were obtained by band-shape analysis of the signals due to the cp hydrogens in the variable-temperature ^1H NMR spectra of **1**–**3**. For clusters **2** and **3**, this analysis was relatively straightforward, because the values of $\Delta G^{\ddagger}$ for the dppf fluxion and the metal-core rearrangement are such that it is possible to obtain ^1H NMR spectra in which there are four cp signals with narrow linewidths (*e.g.* Fig. 1). These spectra correspond to a situation where the dppf fluxion cannot be observed, but the skeletal rearrangement is still fast on the NMR time-scale. As the temperature is raised, the four cp hydrogen signals in the ^1H NMR spectra of each of **2** and **3** coalesce into two peaks, as the

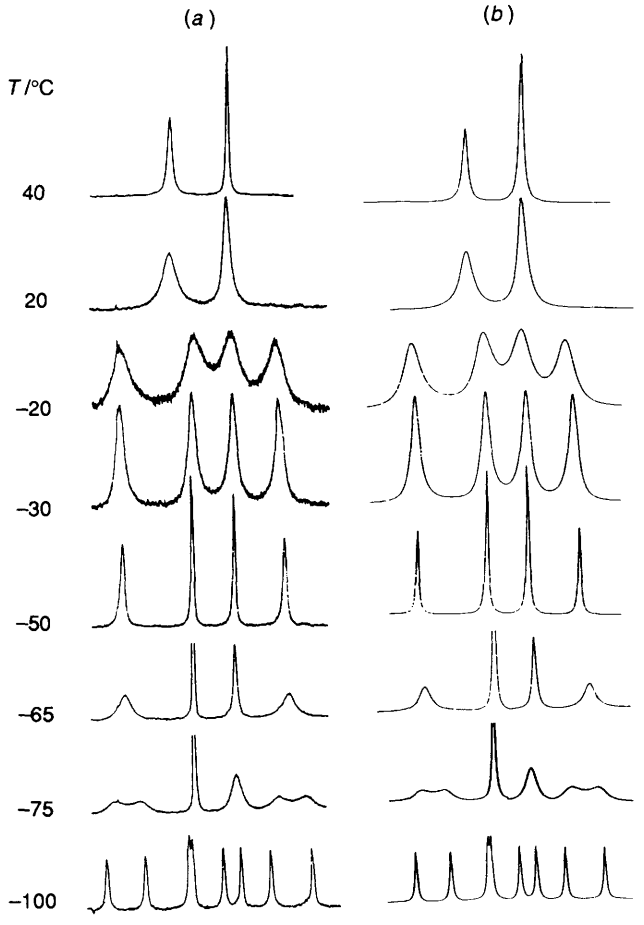

Fig. 1 Observed (*a*) and 'best-fit' computer-simulated (*b*) signals due to the cyclopentadienyl hydrogens in the ^{1}H NMR spectra of $[Ag_2Ru_4(\mu_3\text{-}H)_2(\mu\text{-dppf})(CO)_{12}]$ **2** in CD_2Cl_2

dppf fluxion becomes fast enough to be observed on the NMR time-scale. Good fits between the observed ^{1}H NMR spectra and computer-simulated spectra were obtained between −50 and 40 °C (*e.g.* Fig. 1) and −70 and 40 °C for **2** and **3**, respectively. In the case of the copper-containing cluster **1**, the values of $\Delta G^{\ddagger}$ for the dppf fluxion and the intramolecular metal-core rearrangement are close enough in magnitude for it not to be possible to obtain a ^{1}H NMR spectrum in which there are four cp hydrogen signals with narrow linewidths at any temperature. The assignment of which cp hydrogen peaks were being coalesced by the two different fluxional processes was further complicated by the significant temperature dependence of the chemical shifts of many of the observed signals. Therefore, the two-dimensional exchange spectroscopy (EXSY) ^{1}H NMR spectrum of **1** was recorded at −70 °C to determine unambiguously which cp hydrogen atoms were being exchanged. The observed spectrum (Fig. 2) clearly shows that all of the hydrogen atoms (group 1) which produce signals A, B, F and H are being exchanged and so are all of the hydrogen atoms (group 2) which give rise to peaks C, D, E and G. However, the spectrum also demonstrates that there is no exchange between any of the hydrogens belonging to group 1 and any of those in group 2. As well as revealing details of the hydrogen-atom exchanges, the observed two-dimensional spectrum also provides additional and independent evidence that the cluster undergoes both of the two proposed dynamic processes in solution [2] and it demonstrates that these processes are still fast enough to be detected by two-dimensional EXSY at −70 °C. Unfortunately, this spectrum cannot determine unambiguously which of the hydrogen atoms within each of groups 1 and 2 are exchanged by which of the two fluxional processes. However, utilizing the knowledge previously

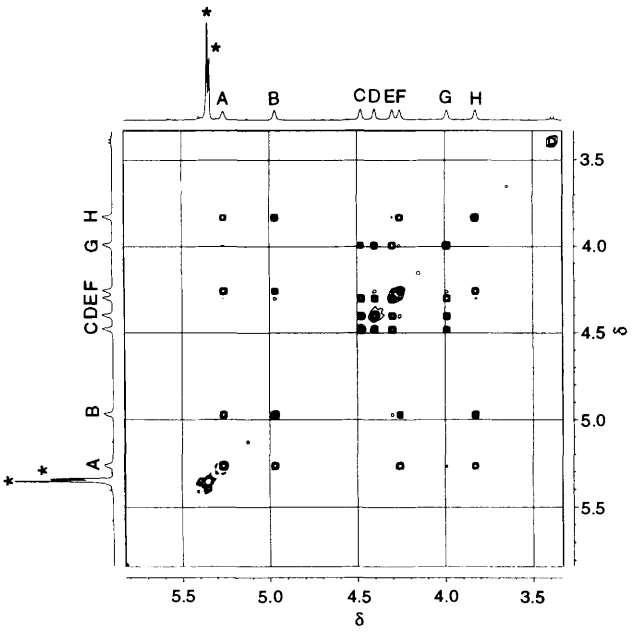

Fig. 2 Signals due to the cyclopentadienyl hydrogens in the two-dimensional EXSY ^{1}H NMR spectrum of $[Cu_2Ru_4(\mu_3\text{-}H)_2(\mu\text{-dppf})(CO)_{12}]$ **1** in CD_2Cl_2 at −70 °C. Signals marked with an asterisk are due to the solvent and the other very small peaks which are visible are either spinning sidebands of the solvent signals or due to trace impurities

obtained from the two-dimensional spectrum of which hydrogen atoms *do not* exchange, inspection of the variable-temperature one-dimensional ^{1}H NMR spectra of **1** reveals which four different pairs of cp hydrogen peaks begin to coalesce when the temperature is raised from −70 °C. Thus, the hydrogen-atom exchanges are A ⟷ B and F ⟷ H for group 1 and C ⟷ D and E ⟷ G for group 2. It is also clear from the one-dimensional ^{1}H NMR spectra that the broadening and beginning of coalescence of the eight cp hydrogen peaks observed between −70 and −50 °C are caused by the above four hydrogen-atom exchanges only. Additional broadening and coalescence of the cp hydrogen signals due to the complete exchange of all of the hydrogen atoms in each of groups 1 and 2 are only visible in the one-dimensional ^{1}H NMR spectra of **1** which were recorded at −46 °C and higher temperatures. Thus, the values of $\Delta G^{\ddagger}$ for the coinage-metal site-exchange process and the dppf fluxion in **1** are clearly different, but also very similar. However, the rate constants for the skeletal rearrangement obtained from the variable-temperature ^{31}P-{^{1}H} NMR spectra of **1** (see below) show that the rate for this process is negligible on the one-dimensional NMR time-scale at temperatures of −50 °C and below. Therefore, the above exchanges of the two cp hydrogen atom pairs in each of groups 1 and 2 and also all of the observed broadening of the eight cp hydrogen signals in the ^{1}H NMR spectra at −50 °C and lower temperatures must only be due to the dppf fluxion. Band-shape analysis was performed on one-dimensional spectra measured between −70 and −50 °C and good fits were obtained in this temperature range. However, to improve the accuracy of the results from this analysis, some values of the rate constants for the dppf fluxion at higher temperatures were also required. Therefore, band-shape analyses of the cp hydrogen signals in the ^{1}H NMR spectra recorded at −46 °C and −43 °C were also performed. Although the variable temperature ^{31}P-{^{1}H} NMR spectra of **1** show that the rate constants for the skeletal rearrangement are not negligible at these temperatures, good fits of the observed ^{1}H NMR spectra were obtained by using the values of these rate constants, which were obtained from the band-shape analysis of the ^{31}P-{^{1}H} NMR spectra, in the computer simulation of the ^{1}H NMR

Table 1 Energy parameters[a] for the fluxional processes observed in solution for the clusters $[MM'Ru_4H_2(\mu\text{-dppf})(CO)_{12}]$ (M = M' = Cu, Ag or Au; M = Cu, M' = Au)

Cluster	$\Delta G^{\ddagger}$/kJ mol^{-1}	$\Delta S^{\ddagger}$/J K^{-1} mol^{-1}	$\Delta H^{\ddagger}$/kJ mol^{-1}
(*a*) 1,1′-Bis(diphenylphosphino)ferrocene fluxion[b]			
1 $[Cu_2Ru_4(\mu_3\text{-}H)_2(\mu\text{-dppf})(CO)_{12}]$	47.0 ± 0.2	10.0 ± 3.0	50.0 ± 0.7
2 $[Ag_2Ru_4(\mu_3\text{-}H)_2(\mu\text{-dppf})(CO)_{12}]$	51.5 ± 0.1	−5.6 ± 2.9	49.8 ± 0.8
3 $[Au_2Ru_4(\mu_3\text{-}H)(\mu\text{-}H)(\mu\text{-dppf})(CO)_{12}]$	48.8 ± 0.2	−3.3 ± 3.7	47.8 ± 0.9
4 $[AuCuRu_4(\mu_3\text{-}H)_2(\mu\text{-dppf})(CO)_{12}]$	49.2 ± 0.2	−9.6 ± 4.5	46.4 ± 1.1
(*b*) Intramolecular rearrangement of the cluster's metal core[c]			
1 $[Cu_2Ru_4(\mu_3\text{-}H)_2(\mu\text{-dppf})(CO)_{12}]$	47.7 ± 0.2[d]	−15.1 ± 6.0[d]	43.2 ± 1.6[d]
2 $[Ag_2Ru_4(\mu_3\text{-}H)_2(\mu\text{-dppf})(CO)_{12}]$	39.9 ± 0.4	−1.8 ± 4.2	39.4 ± 0.8

[a] Calculated at 298.15 K by band-shape analysis of the cyclopentadienyl hydrogen signals in variable-temperature ^{1}H NMR spectra, unless otherwise stated. [b] Fluxional process involves inversion at the phosphorus atoms, together with a twisting of the cyclopentadienyl rings. [c] Band-shape analysis was not possible for cluster **3** and the metal core of **4** is stereochemically rigid in solution, see text. [d] Calculated at 298.15 K by band-shape analysis of variable-temperature ^{31}P-{^{1}H} NMR spectra.

spectra and then varying the magnitude of the rate constant for the dppf fluxion. At temperatures above −43 °C, the band-shapes of the cp hydrogen signals in the ^{1}H NMR spectra were found to be very much more sensitive to changes in the rate constant for the metal-core rearrangement process than to changes in the rate constant for the dppf fluxion. Therefore, sufficiently accurate values of the rate constants for the latter fluxional process could not be obtained at any temperatures above −43 °C.

The energy parameters of the intramolecular metal-core rearrangement for cluster **1** were calculated by band-shape analysis of variable-temperature ^{31}P-{^{1}H} NMR spectra. At −80 °C, two signals are observed in the ^{31}P-{^{1}H} NMR spectrum of **1** and these coalesce into one peak as the temperature is raised. Good fits between the observed and computer-simulated ^{31}P-{^{1}H} NMR spectra were obtained between −50 and 30 °C. The ^{31}P-{^{1}H} NMR spectra of **2** are complicated by ^{107}Ag–^{31}P and ^{109}Ag–^{31}P couplings through one and two bonds, so the energy parameters for the metal-core rearrangement process of **2** were calculated by band-shape analysis of the signals due to the cp hydrogens in the variable-temperature ^{1}H NMR spectra of the cluster. Eight signals are observed at −100 °C and they coalesce into four peaks as the temperature is raised to −50 °C. Good fits were obtained in this temperature region (*e.g.* Fig. 1). The free energy of activation for the skeletal rearrangement process in $[Au_2Ru_4(\mu_3\text{-}H)(\mu\text{-}H)(\mu\text{-dppf})(CO)_{12}]$ **3** is too low for either the low-temperature limiting ^{1}H NMR spectrum or a low-temperature limiting ^{31}P-{^{1}H} NMR spectrum with narrow linewidths to be observed, even at 173 K. Therefore, band-shape analysis of the variable temperature ^{1}H or ^{31}P-{^{1}H} NMR spectra to obtain the energy parameters for the coinage-metal site-exchange process was not possible for **3**. However, the value of $\Delta G^{\ddagger}$ for the metal-core rearrangement in **3** has been previously estimated from the coalescence temperature in the variable-temperature ^{31}P-{^{1}H} NMR spectra as *ca.* 33 kJ mol^{-1} at the coalescence temperature of *ca.* 193 K.[2]

Previous studies on the trimetallic cluster $[AuCuRu_4(\mu_3\text{-}H)_2\{\mu\text{-}Ph_2P(CH_2)_2PPh_2\}(CO)_{12}]$ **5**,[5] which is closely related to **4**, suggest that the metal framework of **4** will be stereochemically rigid in solution. This prediction is confirmed by the hydrido ligand signal in the ambient temperature ^{1}H NMR spectrum of **4**, which consists of a doublet split by ^{31}P–^{1}H coupling (12 Hz) to the phosphorus atom attached to copper. If the two Group 11 metals were undergoing the site-exchange process, the ^{1}H NMR hydrido ligand signal would be expected to be also split by a coupling to the phosphorus atom attached to gold (*e.g.* ref. 2). However, the variable-temperature ^{1}H NMR spectra of **4** do show that the dppf ligand undergoes dynamic behaviour involving inversion of configuration at the phosphorus atoms, together with a concomitant twisting of the cyclopentadienyl rings, as is observed for this ligand in the bimetallic analogues **1**–**3**. At −80 °C, eight signals are observed for the cp hydrogens and two peaks are visible for the hydrido ligands in the ^{1}H NMR spectrum of **4**. As the temperature is raised, the eight cp hydrogen resonances coalesce into four signals and the two hydrido ligand doublets coalesce into a single doublet. These observations are consistent with the dppf fluxion, which creates an effective mirror plane on the NMR time-scale through both of the C_5H_4P units (*cf.* ref. 2). The energy parameters for the dppf ligand fluxion in **4** were obtained by band-shape analysis of the signals due to the cp hydrogens in the variable-temperature ^{1}H NMR spectra of the cluster. Good fits between the observed and computer-simulated spectra were obtained from −80 to 40 °C.

The energy parameters calculated for the clusters **1**–**4** are presented in Table 1. The magnitudes of $\Delta S^{\ddagger}$ for intramolecular fluxional processes in organometallic complexes are frequently found to be between +20 and −20 J K^{-1} mol^{-1} [8] and all of the $\Delta S^{\ddagger}$ values obtained for clusters **1**–**4** lie in this range. This observation is consistent with the proposed intramolecular nature of the dppf fluxion and the metal-core rearrangement process.

It is well established that energies quoted in terms of $\Delta G^{\ddagger}$ values are less prone to systematic errors than the other parameters calculated by band-shape analysis and, therefore, $\Delta G^{\ddagger}$ values are normally used for comparison purposes.[9] It can be seen from Table 1 that the magnitude of $\Delta G^{\ddagger}$ observed for the dppf fluxion is dependent on the nature of the coinage metals bridged by the dppf ligand, but the effect of formally changing the Group 11 metals to which the dppf ligand is bonded does not alter $\Delta G^{\ddagger}$ by a particularly large amount. The $\Delta G^{\ddagger}$ values for the dppf fluxion are almost identical for **3** and **4**, so the formal replacement of a gold atom in **3** by a copper atom in **4** has very little effect on the dynamic behaviour of the dppf ligand. The value of $\Delta G^{\ddagger}$ for the dppf fluxion in the copper-containing cluster **1** is *ca.* 2 kJ mol^{-1} lower than those observed for **3** and **4** and that for the same process in the silver-containing species **2** is *ca.* 2.5 kJ mol^{-1} higher.

The bidentate ligands attached to the coinage metals in the clusters $[M_2Ru_4(\mu_3\text{-}H)_2\{\mu\text{-}Ph_2E(CH_2)_nPPh_2\}(CO)_{12}]$ (M = Cu, E = As or P, n = 1 or 2; M = Cu, E = P, n = 3–6; M = Ag, E = P, n = 2–6), which are structurally closely related to **1**–**4**, are also stereochemically non-rigid in solution.[6] Rapid exchange of the methylene groups in the ligand backbones between the various possible conformations creates an effective mirror plane on the NMR time-scale through the bidentate diphosphine ligand. Thus, the actual effect of this fluxional process is very similar to that caused by the stereochemical non-rigidity of the dppf ligand in **1**–**4**. It has only proved possible to obtain low-temperature-limiting ^{1}H NMR spectra at −100 °C for $[Cu_2Ru_4(\mu_3\text{-}H)_2\{\mu\text{-}Ph_2E(CH_2)_2PPh_2\}(CO)_{12}]$ (E = As or

Table 2 Correlation between the effect of the attached bidentate diphosphine ligand L_2 on the value of $\Delta G^{\ddagger}$ for the metal-core rearrangement process in $[Ag_2Ru_4(\mu_3\text{-}H)_2(\mu\text{-}L_2)(CO)_{12}]$ and the metal-core geometry adopted by $[Au_2Ru_4(\mu_3\text{-}H)(\mu\text{-}H)(\mu\text{-}L_2)(CO)_{12}]$

L_2	$\Delta G^{\ddagger}$	Metal-core geometry
$Ph_2PCH_2PPh_2$	*ca.* 32[a]	Capped square-based pyramid[b]
cis-$Ph_2CH{=}CHPPh_2$	33 ± 1[a]	Capped square-based pyramid[c]
$Ph_2P(CH_2)_2PPh_2$	36.0 ± 0.2[d]	Intermediate between capped trigonal bipyramid and capped square-based pyramid[b]
$Fe(\eta^5\text{-}C_5H_4PPh_2)_2$	39.9 ± 0.4[e]	Intermediate between capped trigonal bipyramid and capped square-based pyramid[e]

[a] Estimated at the coalescence temperature in the observed variable-temperature $^{31}P\text{-}\{^1H\}$ NMR spectra (ref. 6). [b] Ref. 10. [c] Ref. 11. [d] Calculated at 298.15 K by band-shape analysis of variable-temperature $^{31}P\text{-}\{^1H\}$ NMR spectra (ref. 6). [e] This work.

P) and $\Delta G^{\ddagger}$ values of 37 ± 1 kJ mol^{-1} for E = P and 34 ± 1 kJ mol^{-1} for E = As have been calculated by band-shape analysis at 298.15 K for the dynamic behaviour of the bidentate diphosphine ligands in these clusters.[6] The magnitudes of $\Delta G^{\ddagger}$ for the fluxional processes of the bidentate diphosphine ligands in the other clusters must be lower than these values.[6] Therefore, the range of values $\Delta G^{\ddagger}$ of 47.0–51.5 kJ mol^{-1} observed for the dppf fluxion in **1**–**4** is much higher than the magnitudes of $\Delta G^{\ddagger}$ measured for the dynamic behaviour of the bidentate ligands with aliphatic backbones in analogous clusters, which reflects the greater flexibility of the aliphatic $(CH_2)_n$ backbones compared to that of the ferrocenyl unit.

The values of $\Delta G^{\ddagger}$ for the metal-core rearrangements in clusters **1** and **2** which were calculated by band-shape analysis (47.7 ± 0.2 and 39.9 ± 0.4 kJ mol^{-1}) are in good agreement with the magnitudes of $\Delta G^{\ddagger}$ calculated previously for the same process at the coalescence temperature from the coalescence temperatures observed in the variable-temperature $^{31}P\text{-}\{^1H\}$ NMR spectra of the clusters (47 ± 1 and 40 ± 1 kJ mol^{-1}).[2] The values of $\Delta G^{\ddagger}$ for the skeletal rearrangements in **1** and **2** have already been compared with those observed for analogous clusters,[2] but, in view of the previously reported results outlined below for clusters closely related to **2** and **3**, it is of interest to compare the effect of the dppf ligand on the size of $\Delta G^{\ddagger}$ for the metal-core rearrangement in **2** with its influence on the metal-core geometry adopted by **3**. An interesting correlation has previously been found between the effect of the bidentate diphosphine ligands L_2 [L_2 = $Ph_2P(CH_2)_nPPh_2$ (*n* = 1 or 2) or *cis*-$Ph_2PCH{=}CHPPh_2$] on the metal-core geometries adopted by the clusters $[Au_2Ru_4(\mu_3\text{-}H)(\mu\text{-}H)(\mu\text{-}L_2)(CO)_{12}]$ and the influence of the same ligands on the values of $\Delta G^{\ddagger}$ for the metal-core rearrangements of the analogous silver-containing clusters $[Ag_2Ru_4(\mu_3\text{-}H)_2(\mu\text{-}L_2)(CO)_{12}]$.[6] This correlation is summarized in Table 2. When the PPh_3 ligands attached to the gold atoms in $[Au_2Ru_4(\mu_3\text{-}H)(\mu\text{-}H)(CO)_{12}(PPh_3)_2]$ are formally replaced by the bidentate diphosphine ligands $Ph_2PCH_2PPh_2$ or *cis*-$Ph_2PCH{=}CHPPh_2$, the capped trigonal-bipyramidal metal-core structure of the PPh_3-containing cluster is distorted to a capped square-pyramidal skeletal geometry.[10,11] The same formal change of ligands for the silver-containing cluster $[Ag_2Ru_4(\mu_3\text{-}H)_2(CO)_{12}(PPh_3)_2]$ does not change the capped trigonal-bipyramidal skeletal geometry, but it does cause decreases of *ca.* 8 and *ca.* 7 kJ mol^{-1} for L_2 = $Ph_2PCH_2PPh_2$ and *cis*-$Ph_2PCH{=}CHPPh_2$, respectively, in the magnitudes of $\Delta G^{\ddagger}$ for the metal-core rearrangements in the Ag_2Ru_4 metal frameworks of the clusters.[6] These substantial decreases in $\Delta G^{\ddagger}$ for the silver-containing clusters have been explained by proposing that each of the two bidentate diphosphine ligands stabilizes a capped square-pyramidal intermediate in a restricted Berry pseudo-rotation mechanism for the coinage-metal site-exchange process and the size of $\Delta G^{\ddagger}$ is, therefore, reduced in each case.[6] The observed behaviour (Table 2) of the dppe [dppe = $Ph_2P(CH_2)_2PPh_2$] ligand is also consistent with the above hypothesis. When two PPh_3 ligands in $[Au_2Ru_4(\mu_3\text{-}H)(\mu\text{-}H)(CO)_{12}(PPh_3)_2]$ are formally replaced by dppe, the metal-framework structure of the cluster is distorted from capped trigonal bipyramidal towards a capped square-pyramidal geometry, but the extent of the change is very much smaller than that caused by either $Ph_2PCH_2PPh_2$ or *cis*-$Ph_2PCH{=}CHPPh_2$. The dppe ligand does cause the $\Delta G^{\ddagger}$ value for the metal-core rearrangement to be lowered when it formally replaces the two PPh_3 groups in $[Ag_2Ru_4(\mu_3\text{-}H)_2(CO)_{12}(PPh_3)_2]$, but, as expected, this reduction (*ca.* 4 kJ mol^{-1}) is much less than those caused by $Ph_2PCH_2PPh_2$ or *cis*-$Ph_2PCH{=}CHPPh_2$. The results from the single-crystal X-ray diffraction study on cluster **3** (see below) reveal that the dppf ligand in **3** distorts the metal framework of the cluster towards a capped square-based pyramidal geometry and that the metal core structure of **3** is closely similar to that adopted by $[Au_2Ru_4(\mu_3\text{-}H)(\mu\text{-}H)\{\mu\text{-}Ph_2P(CH_2)_2PPh_2\}(CO)_{12}]$. However, it can be seen from Table 2 that the magnitude of $\Delta G^{\ddagger}$ observed for the skeletal rearrangement in **2** is *ca.* 4 kJ mol^{-1} higher than that measured for the analogous cluster containing dppe and it is very similar to the value of 40 ± 1 kJ mol^{-1} which has been previously measured for $[Ag_2Ru_4(\mu_3\text{-}H)_2(CO)_{12}(PPh_3)_2]$.[12] This rather surprising result may, perhaps, be explained by the fact that the dppf ligand is considerably heavier than $Ph_2P(CH_2)_2PPh_2$ and/or the fact that the dppf ligand is considerably less flexible than $Ph_2P(CH_2)_2PPh_2$. Both of these factors are likely to cause the value of $\Delta G^{\ddagger}$ to be higher than might otherwise be expected.

X-Ray crystal structures of $[Au_2Ru_4(\mu_3\text{-}H)(\mu\text{-}H)(\mu\text{-dppf})(CO)_{12}]$ **3** and $[AuCuRu_4(\mu_3\text{-}H)_2(\mu\text{-dppf})(CO)_{12}]$ **4**

The molecular structures of clusters **3** and **4** are shown in Figs. 3 and 4, respectively, and selected bond lengths and angles for the two clusters are summarized in Tables 3 and 4, respectively. In each case, the structures of the dppf-containing clusters **3** and **4** are similar to those previously reported for their dppe analogues $[MM'Ru_4H_2\{\mu\text{-}Ph_2P(CH_2)_2PPh_2\}(CO)_{12}]$ [M = M' = Au **6**[10] or M = Cu, M' = Au **5**[5]].

The structure determined by X-ray diffraction for the trimetallic cluster **4** is consistent with that deduced from the spectroscopic data. The metal skeleton of **4** consists of a tetrahedron of ruthenium atoms, with one face [Ru(1)-Ru(2)Ru(3)] capped by a copper atom and one of the faces of the $CuRu_3$ tetrahedron so formed further capped by a gold atom to give an overall capped trigonal-bipyramidal metal-core geometry. The dppf ligand is attached to the gold and copper atoms and each ruthenium atom is bonded to three essentially linear CO groups. The two hydrido ligands cap the CuRu(1)Ru(2) and CuRu(1)Ru(3) faces of the cluster.

The structure of the bimetallic cluster **3** is reasonably similar to that adopted by **4**, with a second gold atom replacing the copper atom. However, one of the Au–Ru distances

Table 3 Selected bond lengths (Å) and angles (°), with estimated standard deviations (e.s.d.s) in parentheses, for $[Au_2Ru_4(\mu_3\text{-}H)(\mu\text{-}H)(\mu\text{-}dppf)(CO)_{12}]$ **3**

Au(1)–Au(2)	2.901(1)	Au(1)–Ru(1)	2.788(1)
Au(1)–Ru(2)	3.558(2)	Au(1)–Ru(3)	2.796(2)
Au(2)–Ru(2)	2.846(1)	Au(2)–Ru(3)	2.771(1)
Ru(1)–Ru(2)	2.972(2)	Ru(1)–Ru(3)	2.950(1)
Ru(1)–Ru(4)	2.775(2)	Ru(2)–Ru(3)	3.016(1)
Ru(2)–Ru(4)	2.886(2)	Ru(3)–Ru(4)	2.883(2)
Au(1)–P(1)	2.282(5)	Au(2)–P(2)	2.305(4)
Fe–C(cp)	2.019(8)–2.071(11)		
Ru–CO	1.840(18)–1.902(21)		
C–O	1.149(19)–1.194(24)		
Ru(1)–Au(1)–Au(2)	101.9(1)	Ru(2)–Au(1)–Au(2)	51.0(1)
Ru(2)–Au(1)–Ru(1)	54.2(1)	Ru(3)–Au(1)–Au(2)	58.2(1)
Ru(3)–Au(1)–Ru(1)	63.8(1)	Ru(3)–Au(1)–Ru(2)	55.1(1)
Ru(2)–Au(2)–Au(1)	76.5(1)	Ru(3)–Au(2)–Au(1)	59.0(1)
Ru(3)–Au(2)–Ru(2)	64.9(1)	Ru(2)–Ru(1)–Au(1)	76.2(1)
Ru(3)–Ru(1)–Au(1)	58.2(1)	Ru(3)–Ru(1)–Ru(2)	61.2(1)
Ru(4)–Ru(1)–Au(1)	116.1(1)	Ru(4)–Ru(1)–Ru(2)	60.2(1)
Ru(4)–Ru(1)–Ru(3)	60.4(1)	Au(2)–Ru(2)–Au(1)	52.4(1)
Ru(1)–Ru(2)–Au(1)	49.5(1)	Ru(1)–Ru(2)–Au(2)	98.8(1)
Ru(3)–Ru(2)–Au(1)	49.5(1)	Ru(3)–Ru(2)–Au(2)	56.3(1)
Ru(3)–Ru(2)–Ru(1)	59.0(1)	Ru(4)–Ru(2)–Au(1)	93.6(1)
Ru(4)–Ru(2)–Ru(1)	56.5(1)	Ru(4)–Ru(2)–Ru(3)	58.4(1)
Au(2)–Ru(3)–Au(1)	62.8(1)	Ru(1)–Ru(3)–Au(1)	58.0(1)
Ru(1)–Ru(3)–Au(2)	101.1(1)	Ru(2)–Ru(3)–Au(1)	75.4(1)
Ru(2)–Ru(3)–Au(2)	58.7(1)	Ru(2)–Ru(3)–Ru(1)	59.8(1)
Ru(4)–Ru(3)–Au(1)	112.4(1)	Ru(4)–Ru(3)–Au(2)	115.6(1)
Ru(4)–Ru(3)–Ru(1)	56.8(1)	Ru(4)–Ru(3)–Ru(2)	58.5(1)
Ru(2)–Ru(4)–Ru(1)	63.3(1)	Ru(3)–Ru(4)–Ru(1)	62.8(1)
Ru(3)–Ru(4)–Ru(2)	63.0(1)	P(1)–Au(1)–Au(2)	113.1(1)
P(1)–Au(1)–Ru(1)	140.3(1)	P(1)–Au(1)–Ru(2)	143.1(1)
P(1)–Au(1)–Ru(3)	152.6(1)	P(2)–Au(2)–Au(1)	126.2(1)
P(2)–Au(2)–Ru(2)	141.5(1)	P(2)–Au(2)–Ru(3)	151.4(1)
Ru–C–O	165(2)–177(1)		

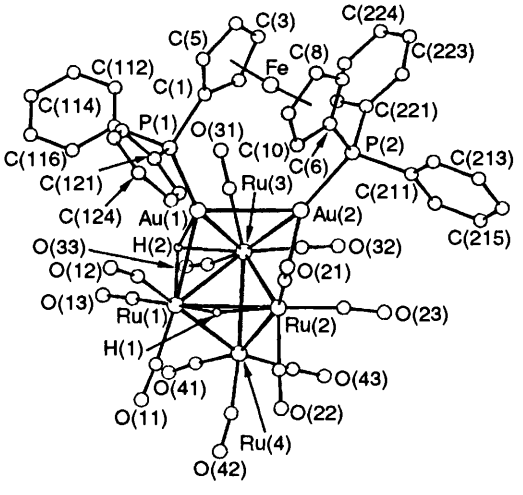

Fig. 3 Molecular structure of $[Au_2Ru_4(\mu_3\text{-}H)(\mu\text{-}H)(\mu\text{-}dppf)(CO)_{12}]$ **3** showing the crystallographic numbering. The carbon atom of each carbonyl group has the same number as the oxygen atom

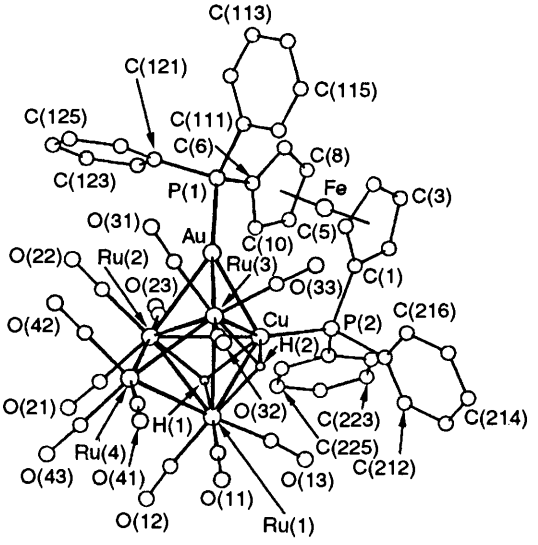

Fig. 4 Molecular structure of $[AuCuRu_4(\mu_3\text{-}H)_2(\mu\text{-}dppf)(CO)_{12}]$ **4** showing the crystallographic numbering. The carbon atom of each carbonyl group has the same number as the oxygen atom

[Au(1)–Ru(2) 3.558(2) Å] is too long for any significant bonding interaction between the two metals, so the stereochemical demands of the dppf ligand distort the metal-core structure of **3** away from capped trigonal bipyramidal towards a capped square-pyramidal skeletal geometry. The metal-framework structure of **3** can, therefore, be best described as intermediate between a capped trigonal bipyramid and a capped square-pyramid. The dppf ligand in **3** is attached to the gold atoms and each ruthenium atom is bonded to three essentially linear CO groups. One hydrido ligand caps the Au(1)Ru(1)Ru(3) face, whereas the other bridges the Ru(1)–Ru(2) edge of the metal framework.

It is of interest to compare quantitatively the metal-core structure of **3** with those adopted by the analogous clusters $[Au_2Ru_4(\mu_3\text{-}H)(\mu\text{-}H)(\mu\text{-}L_2)(CO)_{12}]$ [$L_2 = Ph_2P(CH_2)_nPPh_2$ (n = 1 or 2) or *cis*-$Ph_2PCH{=}CHPPh_2$][10,11] and $[Au_2Ru_4(\mu_3\text{-}H)(\mu\text{-}H)(CO)_{12}(PPh_3)_2]$.[12] It can be seen from Table 5 that the formal replacement of the two PPh_3 ligands attached to the

Table 4 Selected bond lengths (Å) and angles (°), with e.s.d.s in parentheses, for $[AuCuRu_4(\mu_3\text{-}H)_2(\mu\text{-}dppf)(CO)_{12}]$ **4**

Au–Cu	2.641(1)	Au–Ru(2)	2.815(1)
Au–Ru(3)	2.780(1)	Cu–Ru(1)	2.758(2)
Cu–Ru(2)	2.909(2)	Cu–Ru(3)	2.755(1)
Ru(1)–Ru(2)	2.943(1)	Ru(1)–Ru(3)	2.998(1)
Ru(1)–Ru(4)	2.783(1)	Ru(2)–Ru(3)	2.962(1)
Ru(2)–Ru(4)	2.808(1)	Ru(3)–Ru(4)	2.815(1)
Au–P(1)	2.290(3)	Cu–P(2)	2.241(3)
Fe–C(cp)	2.030(8)–2.064(8)		
Ru–CO	1.826(15)–1.920(12)		
C–O	1.141(13)–1.185(14)		
Ru(2)–Au–Cu	64.3(1)	Ru(3)–Au–Cu	61.0(1)
Ru(3)–Au–Ru(2)	63.9(1)	Ru(1)–Cu–Au	114.9(1)
Ru(2)–Cu–Au	60.7(1)	Ru(2)–Cu–Ru(1)	62.5(1)
Ru(3)–Cu–Au	62.0(1)	Ru(3)–Cu–Ru(1)	65.9(1)
Ru(3)–Cu–Ru(2)	63.0(1)	Ru(2)–Ru(1)–Cu	61.3(1)
Ru(3)–Ru(1)–Cu	57.0(1)	Ru(3)–Ru(1)–Ru(2)	59.8(1)
Ru(4)–Ru(1)–Cu	106.4(1)	Ru(4)–Ru(1)–Ru(2)	58.7(1)
Ru(4)–Ru(1)–Ru(3)	58.1(1)	Cu–Ru(2)–Au	54.9(1)
Ru(1)–Ru(2)–Au	104.5(1)	Ru(1)–Ru(2)–Cu	56.2(1)
Ru(3)–Ru(2)–Au	57.5(1)	Ru(3)–Ru(2)–Cu	56.0(1)
Ru(3)–Ru(2)–Ru(1)	61.0(1)	Ru(4)–Ru(2)–Au	112.5(1)
Ru(4)–Ru(2)–Cu	101.8(1)	Ru(4)–Ru(2)–Ru(1)	57.8(1)
Ru(4)–Ru(2)–Ru(3)	58.3(1)	Cu–Ru(3)–Au	57.0(1)
Ru(1)–Ru(3)–Au	104.0(1)	Ru(1)–Ru(3)–Cu	57.1(1)
Ru(2)–Ru(3)–Au	58.6(1)	Ru(2)–Ru(3)–Cu	61.1(1)
Ru(2)–Ru(3)–Ru(1)	59.2(1)	Ru(4)–Ru(3)–Au	113.4(1)
Ru(4)–Ru(3)–Cu	105.6(1)	Ru(4)–Ru(3)–Ru(1)	57.1(1)
Ru(4)–Ru(3)–Ru(2)	58.1(1)	Ru(2)–Ru(4)–Ru(1)	63.5(1)
Ru(3)–Ru(4)–Ru(1)	64.7(1)	Ru(3)–Ru(4)–Ru(2)	63.6(1)
P(1)–Au–Cu	134.4(1)	P(1)–Au–Ru(2)	136.2(1)
P(1)–Au–Ru(3)	155.8(1)	P(2)–Cu–Au	111.2(1)
P(2)–Cu–Ru(1)	133.9(1)	P(2)–Cu–Ru(2)	148.3(1)
P(2)–Cu–Ru(3)	144.0(1)		
Ru–C–O	168(1)–178(1)		

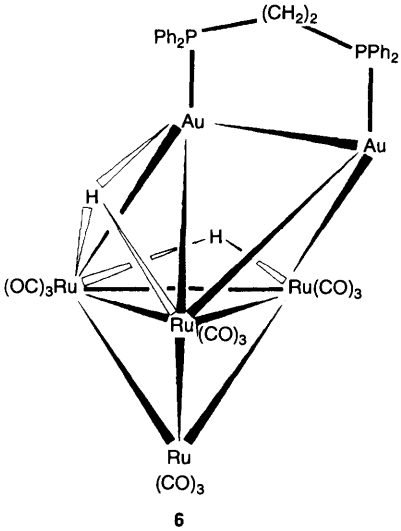

6

gold atoms in $[Au_2Ru_4(\mu_3\text{-}H)(\mu\text{-}H)(CO)_{12}(PPh_3)_2]$ by the bidentate diphosphine ligands distorts the capped trigonal-bipyramidal metal-core structure of the PPh_3-containing species to or towards a capped square-pyramidal skeletal geometry. It has been shown previously[13] that, for clusters containing trigonal bipyramidal or square-pyramidal Au_2Ru_3 units, the degree of distortion from either of the idealized skeletal geometries can be quantified using selected Au–Ru distances. [The atom-numbering scheme was chosen so that Au(2)–Ru(1) > Au(1)–Ru(2) > Au(1)–Ru(3) for each cluster[13] (*cf.* Fig. 3).] The closer Au(1)–Ru(2) and Au(2)–Ru(1) are to being equal, the nearer the Au_2Ru_3 unit in the cluster is to adopting the idealized square-pyramidal geometry. It can be seen from Table 5 that the stereochemical demands of the $Ph_2PCH_2PPh_2$ and *cis*-$Ph_2PCH{=}CHPPh_2$ ligands cause a much greater distortion of the structure of the cluster skeleton away from capped trigonal bipyramidal and towards the idealized capped square-pyramidal geometry than those of the dppe or dppf ligands. The distortions caused by the dppe and dppf ligands are reasonably similar in magnitude and both result in a metal-core structure which is intermediate between capped trigonal bipyramidal and capped square-pyramidal for clusters **6** and **3**. However, the dppf ligand alters the metal framework of **3** slightly further towards a capped square-pyramidal geometry than the dppe ligand does in **6**.

Fig. 5 compares the values of the equivalent metal–metal separations in the metal cores of **3** and **4** with those previously reported for the closely related clusters **6**,[10] **5**[5] and **1**.[2] The Au–Au separation in the dppf cluster **3** [2.901(1) Å] is significantly longer than that in the dppe analogue **6** [2.828(1) Å].[10] The Au–Cu distance in **4** [2.641(1) Å] is larger than that in **5** [2.614(2) Å],[2] but it is intermediate between the magnitude of the Cu–Cu separation in **1** [2.528(2) Å][2] and the length of the Au–Au vector in **5**. The two Au–Ru distances in **4** [2.780(1) and 2.815(1) Å] lie within the range of Au–Ru separations observed in **3** [2.771(1)–2.846(1) Å], but the mean Au–Ru bond length in **4** [2.798(1) Å] is slightly shorter than that in **3** [2.804(2) Å]. The Cu–Ru distances in **4** [2.755(1)–2.909(2) Å] are wider in range than those in the bimetallic copper analogue **1** [2.663(2)–2.830(2) Å] and the trimetallic dppe cluster **5** [2.674(3)–2.822(3) Å]. The M–Ru bonds which are triply bridged by the hydrido ligands in clusters **3** and **4** show an interesting variation relative to their dppe analogues. In **3**, the two Au–Ru bonds associated with the triply bridging hydrido ligand [Au(1)–Ru(1) 2.788(1),

Table 5 Comparison of selected Au–Ru distances in the clusters $[Au_2Ru_4(\mu_3\text{-}H)(\mu\text{-}H)(\mu\text{-}L_2)(CO)_{12}]$ and $[Au_2Ru_4(\mu_3\text{-}H)(\mu\text{-}H)(CO)_{12}(PPh_3)_2]$ to illustrate the varying stereochemical demands of the bidentate diphosphine ligands L_2 [L_2 = dppf, $Ph_2P(CH_2)_nPPh_2$ (n = 1 or 2) or *cis*-$Ph_2PCH{=}CHPPh_2$]

Cluster	Au(1)–Ru(2)/Å	Au(2)–Ru(1)/Å	Metal-core geometry
$[Au_2Ru_4(\mu_3\text{-}H)(\mu\text{-}H)(CO)_{12}(PPh_3)_2]$[a]	2.949	4.730	Capped trigonal bipyramid
$[Au_2Ru_4(\mu_3\text{-}H)(\mu\text{-}H)\{\mu\text{-}Ph_2P(CH_2)_2PPh_2\}(CO)_{12}]$[b]	3.446	4.444	Intermediate between capped trigonal bipyramid and capped square-based pyramid
$[Au_2Ru_4(\mu_3\text{-}H)(\mu\text{-}H)(\mu\text{-dppf})(CO)_{12}]$[c]	3.558	4.419	Intermediate between capped trigonal bipyramid and capped square-based pyramid
$[Au_2Ru_4(\mu_3\text{-}H)(\mu\text{-}H)(\mu\text{-}Ph_2PCH_2PPh_2)(CO)_{12}]$[b]	3.784[d] 3.799[e]	4.123[d] 4.174[e]	Capped square-based pyramid
$[Au_2Ru_4(\mu_3\text{-}H)(\mu\text{-}H)(\mu\text{-}Ph_2PCH{=}CHPPh_2)(CO)_{12}]$[f]	3.827	4.148	Capped square-based pyramid

[a] Ref. 12. [b] Ref. 10. [c] This work. [d] Monoclinic crystalline form. [e] Orthorhombic crystalline form. [f] Ref. 11.

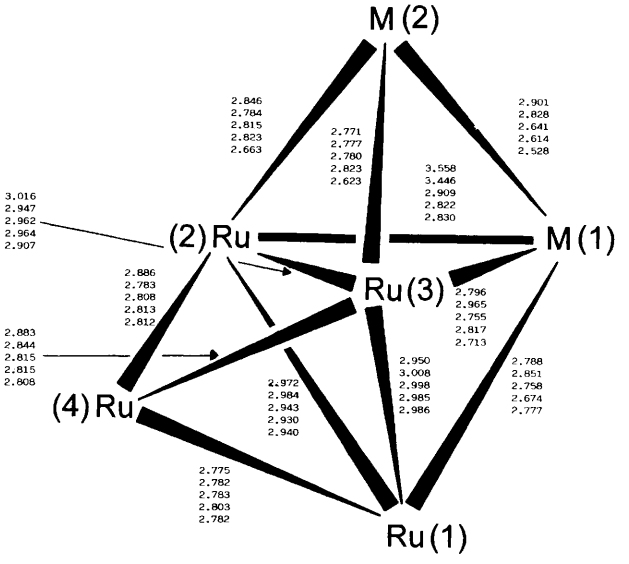

Fig. 5 Comparison of the metal–metal separations (Å) in the metal frameworks of $[MM'Ru_4H_2(\mu\text{-}L_2)(CO)_{12}]$ {M = M' = Au, L_2 = dppf **3** or $Ph_2P(CH_2)_2PPh_2$ **6**; M = Cu [M(1)], M' = Au [M(2)], L_2 = dppf **4** or $Ph_2P(CH_2)_2PPh_2$ **5**; M = M' = Cu, L_2 = dppf **1**}. Distances are given in the following descending order **3**, **6**,[10] **4**, **5**[5] and **1**[2]

Au(1)–Ru(3) 2.796(2) Å] are significantly shorter than the corresponding separations in **6** [Au(2)–Ru(1) 2.851(4), Au(2)–Ru(3) 2.965(4) Å].[9] In the trimetallic cluster **4**, two of the three Cu–Ru bonds are significantly shorter than the other [Cu–Ru(1) 2.758(2), Cu–Ru(3) 2.755(1), Cu–Ru(2) 2.909(2) Å], which is similar to the pattern observed in the bimetallic Cu_2 analogue **1**,[2] but is in marked contrast to the situation observed in the dppe cluster **5**, where two Cu–Ru bonds are longer than the other.[5] The differences within the lengths of the bonds between Group 11 metals and ruthenium discussed above are expected as the relative 'softness' of this type of metal–metal bonding is well established.[7] The mean Ru–Ru distance in **3** [2.914(1) Å] is longer than those in **1** [2.873(3) Å] and **4** [2.885(1) Å], but it is similar to the mean in the digold dppe cluster **6** [2.917(2) Å]. A change in metal-core geometry from capped trigonal bipyramidal in **1** and **4** to intermediate between capped trigonal bipyramidal and capped square-pyramidal in **3** and **6** could account for these variations. Previous studies on Group 11 metal heteronuclear clusters have shown that the lengths of equivalent Ru–Ru vectors which are not capped or bridged by the coinage metals vary very little between closely related clusters[2,6,10,12,14,15] and Fig. 5 shows that this is also the case for Ru(1)–Ru(4), Ru(2)–Ru(4) and Ru(3)–Ru(4) in **6**, **4**, **5** and **1**. However, it is very surprising that the Ru(2)–Ru(4) distance in **3** is *ca.* 0.103–0.073 Å longer than the equivalent separation in any of **6**, **4**, **5** or **1**. Such large variations in equivalent uncapped or unbridged Ru–Ru distances in closely related Group 11 metal heteronuclear clusters are very unusual.[1]

The dppf ligand in each of **3** and **4** bridges the two Group 11 metal atoms (Figs. 3 and 4, respectively). The two cyclopentadienyl rings of the ferrocenyl unit are tilted by 4.45 (in **3**) and 0.77° (in **4**) from being coparallel and they deviate by 9 (in **3**) and 11° (in **4**) from being eclipsed. The corresponding angles reported[2] for **1** are 0.35 and 8°, respectively. The much larger deviation of the cp rings from being coparallel observed for the dppf ligand in **3** is presumably a reflection of the fact that the Au–Au vector in **3** is considerably longer than the Cu–Au bond in **4** or the Cu–Cu separation in **1** (Fig. 5). Although the two C_5 rings in each of clusters **3** and **4** are locked in an approximately eclipsed orientation, the rings are mutually twisted so that the two C–P vectors deviate from one another by 81 (in **3**) and 83° (in **4**). Similar twisting of the C_5 rings (80°) has also been recently observed in the analogous cluster $[Cu_2Ru_4(\mu_3\text{-}H)_2(\mu\text{-dppf})(CO)_{12}]$ **1**.[12] It has been suggested[16] that twisting and/or tilting of the C_5 rings are possible ways in which the dppf ligand can modify its conformation to address any steric constraints imposed when the ligands chelate to metal atoms. Interestingly, even with these conformational changes, the X-ray data show that marked strain around one of the two Group 11 metal–P vectors exists in each of the clusters **3** and **4**. In the digold cluster **3** there is no significant variation between the lengths of the two Au–P vectors [Au(1)–P(1) 2.282(5), Au(2)–P(2) 2.305(4) Å], but the Au–P–C(cp) intercyclic angles are markedly different and this reflects on steric congestion around the Au(1)–P(1) vector. Thus, the angle C(1)–P(1)–Au(1) [119(3)°] is highly distorted away from being tetrahedral, whereas the angle C(6)–P(2)–Au(2) [112(3)°] is near to the ideal tetrahedral angle. This feature is in marked contrast to the situation observed in the analogous clusters $[Au_2Ru_4(\mu_3\text{-}H)(\mu\text{-}H)\{\mu\text{-}Ph_2P(CH_2)_nPPh_2\}(CO)_{12}]$ (n = 1 or 2), in which the corresponding intercyclic angles are similar and both are near to the ideal tetrahedral angle.[10] In cluster **4** the Au–P vector [2.290(3) Å] is significantly longer than the Cu–P vector [2.241(3) Å] and comparison of the intercyclic M–P–C(cp) angles shows a high degree of strain around the Cu–P vector. Thus, the C(6)–P(1)–Au angle [111(2)°] is near to the ideal tetrahedral angle, whereas the C(1)–P(2)–Cu angle is distorted to a larger value [118(2)°]. This situation is similar to that observed in the Cu_2 cluster **1**,[2] but it is in marked contrast to that reported for the trimetallic dppe cluster **5**, where there is no significant variation in the magnitude of M–P (M = Cu or Au) distances and both the intercyclic angles are similar and only slightly distorted from the ideal tetrahedral angle.[5] These results again suggest that the aliphatic backbones of the

Table 6 Crystal-structure determination data for $[Au_2Ru_4(\mu_3\text{-}H)(\mu\text{-}H)(\mu\text{-dppf})(CO)_{12}]\cdot CH_2Cl_2$ **3** and $[AuCuRu_4(\mu_3\text{-}H)_2(\mu\text{-dppf})(CO)_{12}]$ **4***

	3	**4**
Molecular formula	$C_{46}H_{30}Au_2O_{12}P_2Ru_4\cdot CH_2Cl_2$	$C_{46}H_{30}AuCuO_{12}P_2Ru_4$
M	1775.87	1557.47
Crystal dimensions/mm	0.26 × 0.24 × 0.13	0.29 × 0.22 × 0.26
Crystal system	Triclinic	Monoclinic
Space group	$P\bar{1}$ (no.2)	$P2_1/n$
a/Å	13.675(2)	18.274(3)
b/Å	16.999(2)	15.825(2)
c/Å	13.094(2)	16.977(2)
α/°	110.69(2)	90
β/°	112.47(2)	94.61(2)
γ/°	87.99(2)	90
U/Å^3	2613.49	4893.61
D_c/g cm^{-3}	2.257	2.114
Z	2	4
$F(000)$	1668	2968
μ(Mo-Kα)/mm^{-1}	6.90	4.80
No. of reflections measured	8010	7110
No. of unique reflections	7125	6100
Total no. of reflections [$I > 3\sigma(I)$]	6991	5659
Merging R factor	0.044	0.057
Maximum, minimum transmission factors	1.044, 0.844	1.023, 0.866
Number of refined parameters	284	261
R	0.0458	0.0510
R'	0.0456	0.0538
S	1.29	1.40
$\rho_{max,min}$/e Å^{-3}	0.30, −0.48	0.60, −0.57

* Details in common: cell determined from 25 reflections in 2θ range 15–25°, T = 298 K; Philips PW1100 diffractometer, 2θ range 6.0–50.0°, ω–2θ scan mode, step width 0.80°, $F > 6\sigma(F)$, 3 standard reflections with 5% variation in intensity. $R' = \Sigma w^{\frac{1}{2}}(||F_o| - |F_c||)/\Sigma w^{\frac{1}{2}}|F_o|$, $S = [\Sigma w(|F_o| - |F_c|)^2/\Sigma(N_o - N_v)]^{\frac{1}{2}}$.

bidentate diphosphines $Ph_2P(CH_2)_nPPh_2$ (n = 1 or 2) allow more flexibility within the ligand than the ferrocenyl unit of the dppf ligand does in clusters **1**, **3** and **4**.

Although there are no short contact distances between the Group 11 metals and the carbon atoms of the CO ligands in **4**, two such short contacts exist in cluster **3** [Au(1)···C(31) 2.547(19) and Au(1)···C(12) 2.645(13) Å]. This structural feature is present in many Group 11 metal heteronuclear clusters, but the exact nature of the interaction is not well understood.[2,7]

Experimental

All reactions were performed under an atmosphere of dry oxygen-free nitrogen, using Schlenk-tube techniques.[17] Solvents were freshly distilled under nitrogen from the usual drying agents immediately before use. Light petroleum refers to that fraction of b.p. 40–60 °C. Established methods were used to prepare the clusters $[M_2Ru_4H_2(\mu\text{-dppf})(CO)_{12}]$[2] and the compound $[AuCl(SC_4H_8)]$.[18] Product separation was performed on BDH alumina (Brockman activity II). Infrared spectra were recorded on a Perkin-Elmer 881 spectrophotometer. The NMR spectroscopic data for **4**, which are quoted below, were obtained from spectra recorded on a Bruker AC 300 (^{1}H) or DRX 400 (^{31}P-{^{1}H}) spectrometer. Chemical shifts for the ^{31}P-{^{1}H} spectrum are relative to 85% aqueous H_3PO_4 (external).

Synthesis of the trimetallic cluster $[AuCuRu_4(\mu_3\text{-}H)_2(\mu\text{-dppf})(CO)_{12}]$ 4

A dichloromethane solution (50 cm^3) of $[AuCl(SC_4H_8)]$ (0.06 g, 0.19 mmol) was added dropwise to a stirred dichloromethane (100 cm^3) solution of the bimetallic cluster compound $[Cu_2Ru_4(\mu_3\text{-}H)_2(\mu\text{-dppf})(CO)_{12}]$ **1** (0.40 g, 0.28 mmol) over a period of 1 h. After removal of the solvent under reduced pressure, the crude residue was dissolved in dichloromethane–light petroleum (2:1) and chromatographed on an alumina column (*ca.* 20 × 3 cm). Elution with dichloromethane–light petroleum (2:1) produced a dark red fraction containing a trace amount of the bimetallic cluster $[Au_2Ru_4(\mu_3\text{-}H)(\mu\text{-}H)(\mu\text{-dppf})(CO)_{12}]$ **3** [ν_{max}(CO) identical to data in ref. 2], followed by a red fraction containing the trimetallic cluster $[AuCuRu_4(\mu_3\text{-}H)_2(\mu\text{-dppf})(CO)_{12}]$ **4**. After removal of the solvent under reduced pressure from this second main fraction, crystallization of the residue from dichloromethane–light petroleum afforded dark red microcrystals of the product **4** {0.12 g, 41% yield based on the amount of the complex $[AuCl(SC_4H_8)]$ taken for reaction}, m.p. 185–188 °C (decomp.) (Found: C, 35.2; H, 2.0. $C_{46}H_{30}AuCuFeO_{12}P_2Ru_4$ requires C, 35.5; H, 1.9%). ν_{max}(CO) at 2071s, 2035vs, 2022vs, 2009s, 1988 (sh), 1977m (br) and 1947m (br) cm^{-1} (CH_2Cl_2). NMR (CD_2Cl_2): ^{1}H (+30 °C), δ −17.53 [d, 2 H, J(PH) 12, μ_3-H], 4.14 (s, 2 H, C_5H_4), 4.27 (s, 2 H, C_5H_4), 4.51 (br s, 2 H, C_5H_4), 4.74 (br s, 2 H, C_5H_4) and 7.32–7.64 (m, 20 H, Ph); ^{1}H (−80 °C), δ −17.57 [d, 1 H, J(PH) 11, μ_3-H], −18.05 [d, 1 H, J(PH) 14, μ_3-H], 3.83, 3.91, 4.08 4.14, 4.31, 4.46, 4.90, 5.27 (8 × s, 1 H each, C_5H_4) and 7.24–7.92 (m, 20 H, Ph); ^{31}P-{^{1}H} (−80 °C), δ 66.3 (s, 1P, PAu) and −0.6 (s, 1 P, PCu).

Variable-temperature NMR spectroscopic studies

The variable-temperature ^{1}H NMR spectra of clusters **2**–**4** for computer simulation were measured on a Bruker AC 300 spectrometer operating at 300.13 MHz. The variable-temperature NMR spectra of cluster **1** for computer simulation were recorded on a Bruker DRX 400 instrument operating at 400.13 and 161.98 MHz, respectively, for the ^{1}H and ^{31}P-{^{1}H} NMR spectra. The two-dimensional EXSY ^{1}H NMR spectrum of **1** was recorded on a Bruker DRX 400 spectrometer with a mixing time (τ) of 0.5 s. All spectroscopic measurements were performed on CD_2Cl_2 solutions of the clusters **1**–**4**. Samples were prepared under an atmosphere of dry, oxygen-free nitrogen in standard 5 mm NMR tubes. A standard B-VT1000 (AC 300) or a Eurotherm B-VT2000 (DRX 400) variable-temperature unit was used to control the probe temperature. The temperatures are considered accurate to ± 1 °C.

Rate data were obtained from band-shape analysis of

variable-temperature ^1H or $^{31}P-\{^1H\}$ NMR spectra using a modified version of the standard DNMR program[19] of Kleier and Binsch.[20] Activation parameters based on experimental rate data were calculated using the THERMO program.[19]

Crystal-structure determination of $[MM'Ru_4H_2(\mu\text{-dppf})(CO)_{12}]$ [M = M′ = Au 3 or M = Cu, M′ = Au 4]

Suitable crystals of the clusters **3** and **4** were grown from dichloromethane–light petroleum by slow layer diffusion at −20 °C.

Details of crystal and data collection parameters and refinement data are summarized in Table 6. The methods of data collection and processing used for clusters **3** and **4** have been described previously.[21] For both clusters, the positions of the metal atoms were deduced from a Patterson synthesis. The remaining non-hydrogen atoms were located from subsequent Fourier-difference syntheses.[22] Absorption corrections were applied to the data after initial refinement of the isotropic parameters of all of the non-hydrogen atoms.[23] Although the two hydrido ligands in the structure of each of **3** and **4** were not located directly from the data, suitable positions were obtained from potential-energy minimization calculations.[24] These hydrogen atoms were then included in the structure-factor calculations, with fixed thermal parameters of 0.08 Å^2, but their parameters were not refined. The carbon atoms of the phenyl and the cyclopentadienyl rings in both structures were grouped together as rigid hexagons [d(C–C) = 1.395 Å] and pentagons [d(C–C) 1.420 Å], respectively. The hydrogen atoms were included in geometrically idealized positions and constrained to 'ride' on the relevant carbon atoms [d(C–H) = 1.08 Å] with common group isotropic thermal parameters of 0.08 Å^2, which were not refined. Anisotropic thermal parameters were assigned to the metal and the phosphorus atoms in **3** and **4** and the chlorine atoms of the solvent molecule in **3** during the final cycles of full-matrix refinement which converged at R and R' values of 0.0458 and 0.0456 for **3** and 0.0510 and 0.0538 for **4**, respectively, with weights of $w = 1/\sigma^2(F_o)$ assigned to individual reflections.

Complete atomic coordinates, thermal parameters and bond lengths and angles have been deposited at the Cambridge Crystallographic Data Centre. See Instructions for Authors, *J. Chem. Soc., Dalton Trans.*, 1996, Issue 1.

Acknowledgements

We thank Drs. Andrew Gelling and Daniel Fletcher for helpful discussions, Exeter University for a studentship (S. A. W.), Johnson Matthey plc for a generous loan of $HAuCl_4$, Mr. Roger Lovell for technical assistance and Mr. Graham Luscombe for producing the structural formulae and Fig. 4.

References

1 Part 19, T. Adatia and I. D. Salter, *Polyhedron*, 1996, **15**, 597.
2 I. D. Salter, S. A. Williams and T. Adatia, *Polyhedron*, 1995, **14**, 2803.
3 S. M. Draper, C. E. Housecroft and A. L. Rheingold, *J. Organomet. Chem.*, 1992, **435**, 9.
4 S. T. Chacon, W. R. Cullen, M. I. Bruce, O. bin Shawkataly, F. W. B. Einstein, R. H. Jones and A. C. Wilks, *Can. J. Chem.*, 1990, **68**, 2001.
5 S. S. D. Brown, I. D. Salter and T. Adatia, *J. Chem. Soc., Dalton Trans.*, 1993, 559.
6 C. P. Blaxill, S. S. D. Brown, J. C. Frankland, I. D. Salter and V. Šik, *J. Chem. Soc., Dalton Trans.*, 1989, 2039.
7 I. D. Salter, in *Comprehensive Organometallic Chemistry II*, eds. G. Wilkinson, F. G. A. Stone and E. W. Abel, Pergamon, Oxford, 1995, vol. 10, p. 255.
8 B. E. Mann, in *Comprehensive Organometallic Chemistry*, eds. G. Wilkinson, F. G. A. Stone and E. W. Abel, Pergamon, Oxford, 1982, ch. 20.
9 E. W. Abel, S. K. Bhargava and K. G. Orrell, *Prog. Inorg. Chem.*, 1984, **32**, 1.
10 S. S. D. Brown, I. D. Salter, A. J. Dent, G. F. M. Kitchen, A. G. Orpen, P. A. Bates and M. B. Hursthouse, *J. Chem. Soc., Dalton Trans.*, 1989, 1227.
11 T. Adatia, *Acta Crystallogr., Sect. C*, 1993, **49**, 1926.
12 M. J. Freeman, A. G. Orpen and I. D. Salter, *J. Chem. Soc., Dalton Trans.*, 1987, 379.
13 A. G. Orpen and I. D. Salter, *Organometallics*, 1991, **10**, 111.
14 S. S. D. Brown, I. D. Salter and L. Toupet, *J. Chem. Soc., Dalton Trans.*, 1988, 757.
15 S. S. D. Brown, P. J. McCarthy, I. D. Salter, P. A. Bates, M. B. Hursthouse, I. J. Colquhoun, W. McFarlane and M. Murray, *J. Chem. Soc., Dalton Trans.*, 1988, 2787.
16 C. E. Housecroft, S. M. Owen, P. R. Raithby and B. A. M. Shaylih, *Organometallics*, 1990, **9**, 1619 and refs. therein.
17 D. F. Shriver, *The Manipulation of Air-Sensitive Compounds*, McGraw-Hill, New York, 1969.
18 R. Uson and A. Laguna, *Organomet. Synth.*, 1986, **3**, 315.
19 V. Šik, Ph.D. Thesis, University of Exeter, 1979.
20 D. A. Kleier and G. Binsch, *J. Magn. Reson.*, 1970, **3**, 146; DNMR3, Program 165, Quantum Chemistry Exchange, Indiana University, 1970.
21 M. K. Cooper, P. J. Guerney and M. McPartlin, *J. Chem. Soc., Dalton Trans.*, 1982, 757.
22 G. M. Sheldrick, SHELX 76, Program for Crystal Structure Determination, University of Cambridge, 1976.
23 N. Walker and D. Stuart, DIFABS, *Acta Crystallogr., Sect. A*, 1983, **39**, 158.
24 A. G. Orpen, *J. Chem. Soc., Dalton Trans.*, 1980, 2509.

Received 4th August 1995; *Paper* 5/07075I